Contents lists available at ScienceDirect

Scripta Materialia

journal homepage: www.elsevier.com/locate/scriptamat



Core effect of local atomic configuration and design principles in Al_xCoCrFeNi high-entropy alloys



Yu-Chia Yang^a, Cuixia Liu^b, Chun-Yu Lin^a, Zhenhai Xia^{a,*}

- ^a Department of Materials Science and Engineering, University of North Texas, Denton, TX 76203, USA
- ^b School of Materials Science and Engineering, Xi'an Technological University, Xi'an 720072, China

ARTICLE INFO

Article history: Received 22 August 2019 Revised 1 November 2019 Accepted 8 November 2019

Keywords:
High entropy alloys
DFT calculation
Design principles
Stacking fault energy
Local atomic configuration

ABSTRACT

High-entropy alloys (HEAs) are known to have four core effects leading to superior properties over traditional alloys. In this paper, we investigate an additional core effect, local atomic configuration, due to inherent variations of local chemical composition at the nanoscale. The stacking fault and twin formation energies of Al_xCoCrFeNi HEAs, calculated with density functional theory methods, show large variations and even negative energies due ro the local atomic configurations. A design principle is proposed to predict the mechanical properties of the HEAs. The effect of temperature on stacking fault energy is also determined, which is consistent with experimental results.

© 2019 Acta Materialia Inc. Published by Elsevier Ltd. All rights reserved.

High-entropy alloys (HEAs), which contain at least four components without major elements, have become one of the most popular metallic materials in the past twenty years owing to thier excellent mechanical properties, good high-temperature stability and high resistance to wear and corrosion [1-5]. Generally, these outstanding properties can be attributed to four core effects, namely high-entropy, severe-lattice-distortion, sluggish diffusion and cocktail [3,4]. From the viewpoint of thermodynamics, the competition between enthalpy and entropy determines the phase stability. The large configurational entropy resulting from the multiple components stabilizes the solid solution without the formation of intermetallic compounds. Therefore, the high-entropy ensures the higher propensity to maintain single-phase structures. Other major advantages of HEAs are the high strength and hardness, and such good mechanical properties stem from the severe-lattice-distortion effect. The movement of dislocation is hindered by the distorted lattice due to the difference in size for multiple components. The cocktail effect states that there are mutual interactions between components. For instance, strong B2 phase is formed in Al_xCoCrFeNi. For the sluggish diffusion effect, Tsai et al. [6] employed the quasi-chemical model and successfully demonstrated that the diffusion and phase transformation rate decreased with increasing the number of components in the HEA. In other words, the migration of atoms or vacancies was hindered due to the higher fluctuation of lattice potential energy resulted

from significant variations of the nearest neighboring bonding during the atomic migration. They derived that the fluctuation of lattice potential energy was related to the probability of atomic configuration (entropy) and cohesive energy.

In addition to the four core effects, there is an inherent variation of local chemical composition in HEAs, which may play an important role in determining their mechanical behaviors. While HEAs form a single phase (e.g., FCC or BCC) structure, the local chemical composition varies significantly at the nanoscale, resulting in nanoscale cluster-like structures or local atomic configurations (LACs). These locally existing clusters would strongly affect the movement of dislocation and twin formation, consequently enhancing the mechanical properties of the HEAs. In the present work, the LACs in HEAs were systemematically investigated as an independent effect with the density functional theory (DFT) calculations. Al_xCoCrFeNi HEA was chosen as a model alloy, owing to its outstanding mechanical properties and the dual-phase characteristic, allowing more possible strengthening mechanisms to be applied [7-11]. We demonstrated that the effect of the LACs in Al_xCoCrFeNi HEA could lead to not only negative stacking fault energy (SFE) and negative twin formation energy (TFE), but also notable fluctuations in SFE and TFE in local regions. Through the calculations of the SFEs for different LACs, a design principle was developed to predict the HEAs with high mechanical properties. The effect of temperature on SFE was also determined, which was consistent with experimental results.

DFT calculations were performed by the Vienna Ab inito Simulation Package (VASP version 5.4.1) [12–14] based on a plane-wave

^{*} Corresponding author.

E-mail address: zhenhai.xia@unt.edu (Z. Xia).

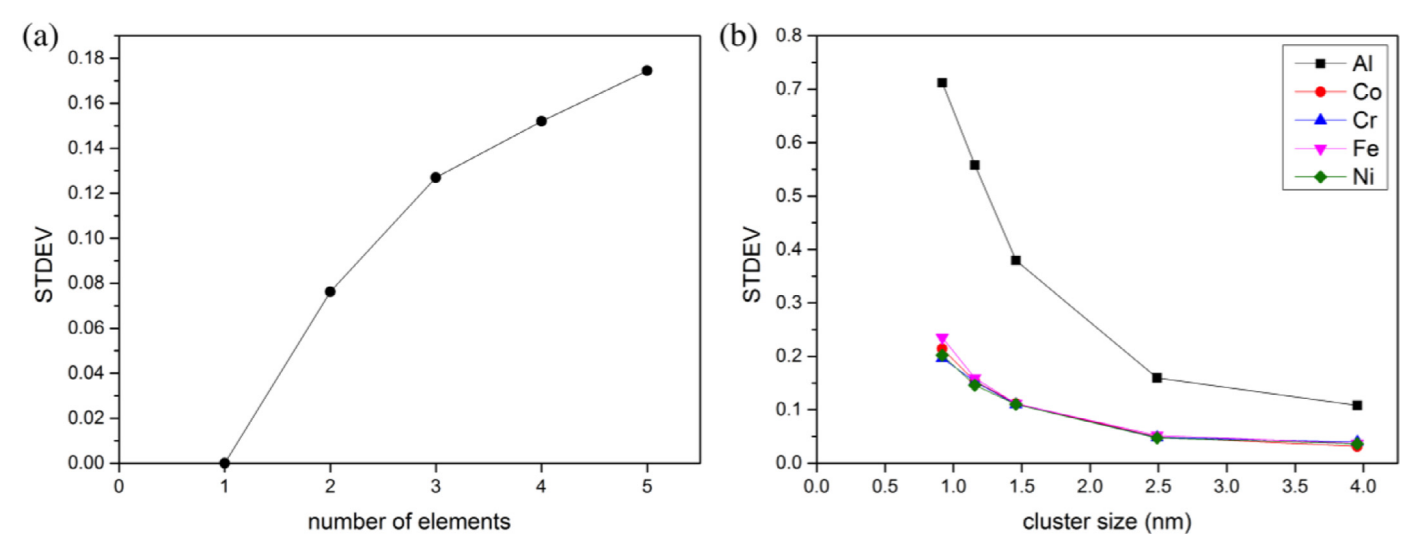


Fig. 1. Inherent chemical composition variations in Al_{0.1}CoCrFeNi HEA. Standard deviation (STDEV) of the composition as functions of (a) the number of principal elements, and (b) cluster size in the HEA.

pseudopotential approach and the Projector Augmented Wave (PAW) method [15,16] was implemented. The generalization gradient approximation (GGA) option, Perdew-Burk-Ernzerhof (PBE) [17], was employed as the exchange-correlation function, and the valence electrons for Al, Co, Cr, Fe and Ni were 3, 9, 6, 8 and 10, respectively. The cut-off energy of plane waves was 400 eV and a $4 \times 4 \times 4$ Monkhorst k-point grid [18] was used. The selection criteria for both of the cut-off energy and k-point mesh were based on the variation of the total energy converging to the order of 1 meV/atom. For our calculations, the boundaries were periodic and the spin polarization was included. There were 144 atoms with 5 species randomly assigned to the FCC lattice points and a structure relaxation was performed in order to obtain the ground state energies for different models. The energy tolerance was set to 10^{-4} eV between two successive electronic steps. All these settings were applied to calculate the lattice constant, cohesive energy, vacancy energy, SFE and TFE, which are described in details in Support Information.

 Al_x CoCrFeNi HEAs (x = 0, 0.1, 0.3 and 0.5) were generated by randomly assigning principal elements in FCC lattice such that the elements were distributed uniformly in the alloy. In spite of the uniform distribution at the large scale, there is an inherent variation of chemical composition at the nanoscale, as shown in Fig. 1. These chemical composition variations or LACs increase with increasing the number of principal elements (Fig. 1a), i.e., the entropy. The variations in chemical composition reduce with increasing the selected domain size. The large variations at the nanoscale lead to an uneven distribution of principal elements. Each local domain could be considered as a cluster with different chemical composition and local atomic configuration. As shown in Fig. 1b, the size of the cluster with large difference of LACs is around 1–2 nm. This pronounced composition fluctuation in the CrFeCoNiPd alloy were observed experimentally and such fluctuation leads to new strengthening mechanisms in HEAs [19]. Therefore, the LACs could be considered as a new core effect in HEAs.

According to the conclusions of Tsai et al. [6], the fluctuation of lattice potential energy was determined by the probability of atomic configuration and the lattice potential energy. Therefore, we calculated the lattice constant, and vacancy and cohesive energies for $Al_{0.1}$ CoCrFeNi. The lattice constants of the HEA (Fig. S1) are in good agreement with the experimental results measured at room temperature for x=0, 0.1, 0.3 and 0.5. [8]. The vacancy energies of the HEA and pure metals are comparable for Co, Fe and Ni except for Al and Cr (Fig. S2b). The higher vacancy en-

ergy for Al in the HEA may be attributed to the local bonding environments, or LACs. Basically, the bonding environments of Al atoms in HEAs are totally different from pure Al. In the HEA, Al is surrounded by the transition metals with the unpaired electrons from d-orbitals, making the metallic bond with Al stronger than that in pure Al. Hence, more energy is needed to form an Al vacancy in the HEA. On the other hand, the low vacancy energy of Cr in HEA is probably due to the fact that Cr is the only elemental solid showing antiferromagnetic ordering at room temperature. As shown in Fig. S3a, the average vacancy energy from the DFT calculations is comparable to the energy calculated by the rule of mixtures: $E_{vac} = f_{Al}E_{Al} + f_{Co}E_{Co} + f_{Cr}E_{Cr} + f_{Fe}E_{Fe} + f_{Ni}E_{Ni}$, where f is the molar fraction, E is the vacancy energy for pure metals calculated by DFT, and subscripts are the elements. Similar results were obtained for the cohesive energy (Fig. S3b). Such results demonstrate that the lattice energy is not improved by the formation of high-entropy system and hence the atomic configuration is the only reason contributing to the sluggish diffusion and structural stability in Al_xCoCrFeNi. Thus, the most critical issue about enhancing the structural stability is the atomic configuration, and the LAC, due to the inherent composition difference in the nanoscale clusters, would strongly influence the mechanical properties of the

For conventional metals and alloys, SFE has been demonstrated as an effective indicator to determine the mechanical properties. For instance, copper and steels with low SFE exhibit twinninginduced plasticity (TWIP) during deformation [20,21]. TWIP steel shows huge elongation and high fracture toughness due to the occurrence of mechanical twinning hindering the dislocations and increasing the strain hardening rate. Similarly, SFE and TFE are reported that they are likely to be two of the most influential factors in HEAs [22-24]. For HEAs, the SFE and TFE not only depend on the components, but also are very sensitive to LACs. The SFE and TFE were calculated using the models shown in Fig. 2a and b, repectively. Fig. 2c and d shows the wide distribution of SFE and TFE for Al_xCoCrFeNi ranging from negative to positive values for different atomic distributions (i.e., different LACs) with the same chemical composition. Thus, the LAC has enormous influence on the SFE and TFE for HEAs. In addition to the wide range of energy distributions, there is an increasing trend of SFE and TFE as a function of the amount of Al (Fig. 2c and d). The increasing energy competes with the precipitation strengthening because the propensity of twinning decreases as more Al is added. Therefore, it is possible to find the best composition with satisfying toughness and strength.

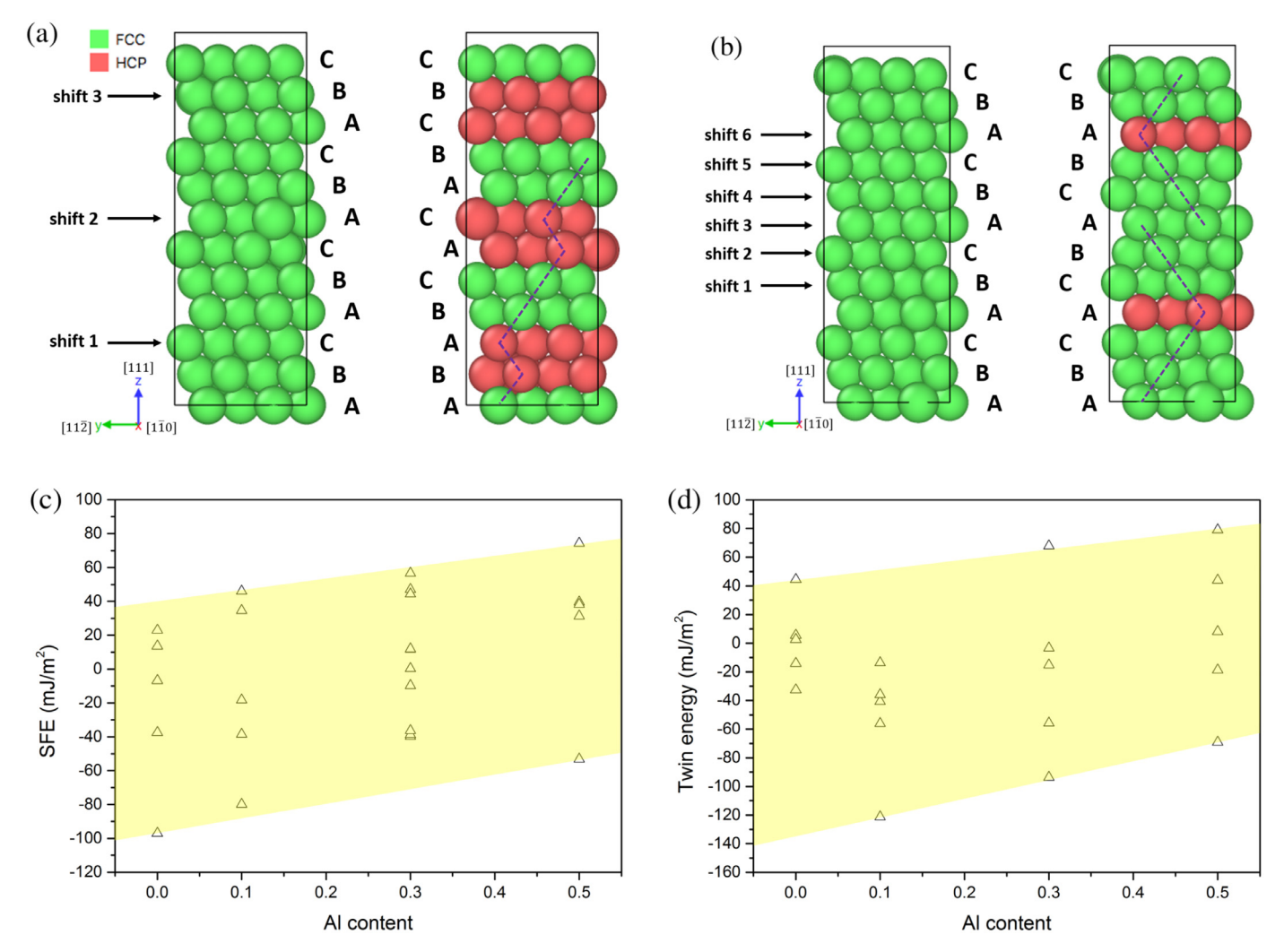


Fig. 2. (a) A perfect model (left) and a model containing 3 stacking faults (right). The periodic boundary condition is maintained by introducing three layers of stacking faults and the dash lines refer to the atomic arrangements changed by stacking faults. (b) A perfect model (left) and a model containing two twins (right). The periodic boundary condition is maintained and two twins are separated by an equal distance with 6-plane displacements. The dash lines represent the atomic arrangements of twin structure. Wide distribution of (c) SFEs and (d) TFEs for Al_xCoCrFeNi due to different local atomic configurations. The yellow band represents the general trend of increasing SFE or TFE with increasing the amount of Al. (For interpretation of the references to color in this figure legend, the reader is referred to the web version of this article.)

The negative SFE is attributed to the HCP structure in the HEA having lower free energy than the FCC structure for a specific LAC. Because of the composition variations in local areas, HCP may be more stable than FCC in some domains and the FCC-to-HCP transformation should be spontaneous once it is triggered. The effect of LAC on SFE distribution was determined and Fig. 3(a)-(f) show the SFE and elemental distributions for Al_{0.1}CoCrFeNi. As shown in Fig. 3(a), some peaks and valleys are formed in a region that is only about 31 nm². The highest SFE is 46.09 (mJ/m²) while the lowest one is -79.78 (mJ/m²). The result demonstrates that SFE can have extreme changes at the nanoscale for the alloys with various components and such variations are induced by the chemical compositions variation or LAC. The extreme SFE variations could result in the local dissociation of dislocation in the areas with low or negative SFE. This prediction has been proved by the experimental results on dislocations in HEAs. It was observed in in-situ TEM straining experiments that some dislocations dissociated into leading and trailing partials due to the pronounced fluctuation of chemical composition [19]. It was argued that this dislocation dissocation can only occur when SFE is extremely low or negative. This provides a direct evidence that SFE and dislocation motion are significantly influenced by the LACs.

To analyze the effect of LAC on SFE in a more specific way, the variations of the constituent elements for Al_{0.1}CoCrFeNi at the nanoscale were collected and the elemental distributions were presented in the same region as in the SFE distribution. According to the SFE and composition distributions in Fig. 3b–f, Al and Ni generally show positive correlations with SFE (Higher concentration of Al and Ni results in higher SFE, and vice versa) although SFE is simultaneously affected by all of the constituent elements. However, the local region with low Co concentration has more or less coorespondence with the region where there are SFE peaks. More detailed correlation coefficients regarding the SFE and the amounts of elements will be discussed later.

Although there is a large variation in SFE due to LACs, it is expected that it will become smaller with increasing the domain size, and the SFE eventually converges to a certain value. To test the convergence, we built a series of models of $Al_{0.1}$ CoCrFeNi HEA with different sizes. For the models larger than the size with 144 atoms, they were built by repeatedly staking the model with 144 atoms. Fig. S4a shows the SFE as a function of the domain size. With increasing the number of atoms in the models, the SFE gradually converges to -9.12 mJ/m^2 , and the standard deviation of the SFE dramatically decreases as well (Fig. S4b). For $Al_{0.1}$ CoCrFeNi HEA,

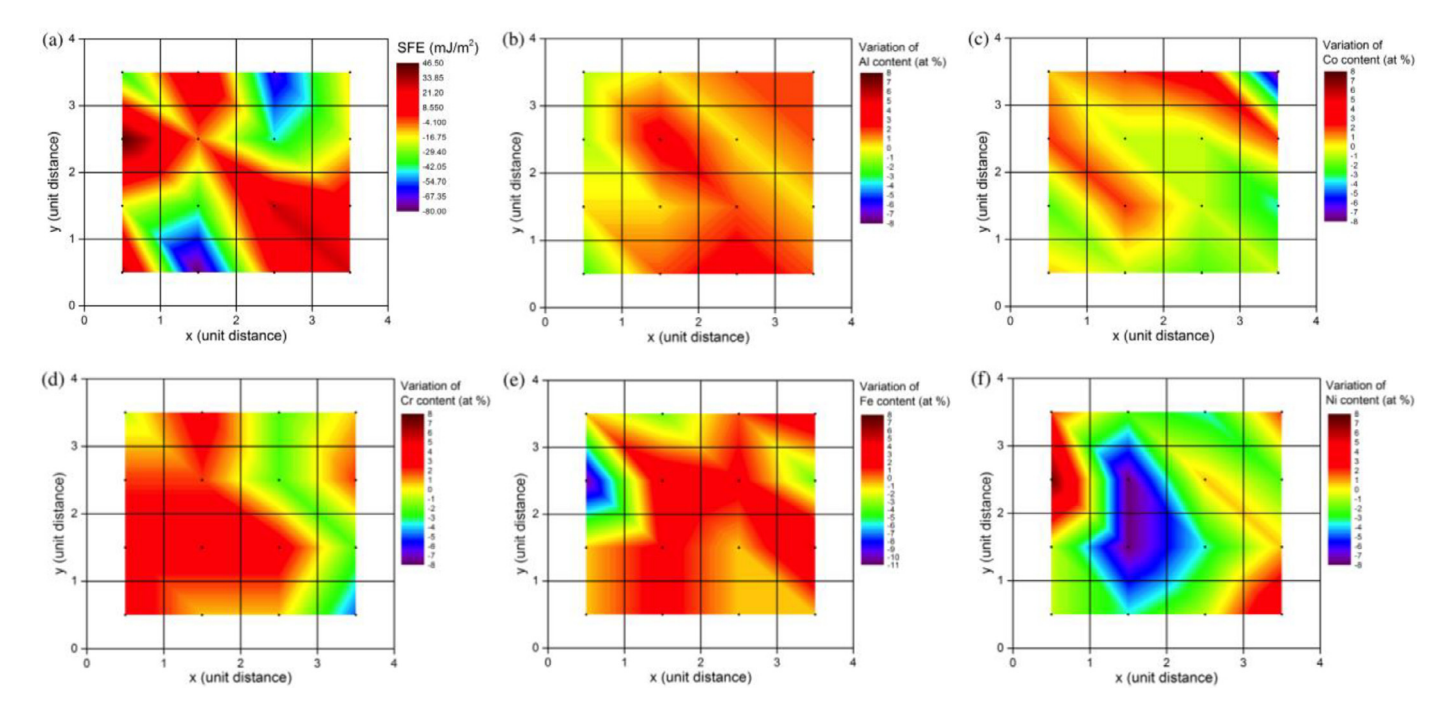


Fig. 3. (a) SFE distribution showing intensive collection of peaks and valleys within a small area. The unit distance is selected to 1.4 nm, because there are three layers of stacking faults within a model and the area of three stacking faults is 1.96 nm². The elemental distributions for (b) Al, (c) Co, (d) Cr, (e) Fe and (f) Ni. The distributions of Al and Ni have somewhat positive correlations with SFE distribution while Co distribution shows more of less negative correlation with SFE.

the convergent domain size is about 2 nm (~600 atoms), which is consistent with the domain size of LACs (Fig. 1b).

Since the composition in stacking fault area mainly determines the SFE of HEAs, we have calculated the free energy for both FCC and HCP structures. The calculation results (Fig. 4a) confirm the hypothesis that the HCP is more stable than FCC in some areas, leading to the negative SFE. We further calculated the SFE with the results for HCP and FCC by assuming there were two HCP layers embedded in the FCC structure. As shown in Fig. 4b, the calculated SFE agrees well with the DFT calculations. Thus, an alternative and convenient way to evaluate average SFE is to calculate the free energy of HCP and FCC structures independently.

Since the SFE is closely related to the local chemical compositions or LACs, it is possible to use these variations with limited calculations to predict the HEA with low SFE. We have randomly generated 16 models with different atomic distributions and determined their SFEs and the correspending chemical composition in stacking faults for Al_{0.1}CoCrFeNi. Assuming that the relationship between the SFE and the chemical composition in stacking faults is linear, the SFE for different compositions can be predicted by the equation:

$$SFE = a_{Al}x_{Al} + a_{Co}x_{Co} + a_{Cr}x_{Cr} + a_{Fe}x_{Fe} + a_{Ni}x_{Ni}$$
 (1)

where a_i is the SFE coefficient for species i and x_i is the molar fraction of species i in a stacking fault. The coefficients were determined from the DFT results and the final equation to evaluate the SFE was derived as:

$$SFE = 200.3x_{Al} - 102.54x_{Co} - 128.64x_{Cr} + 47.27x_{Fe} + 133.45x_{Ni}$$
 (2)

According to Eq. (2), Al, Fe and Ni raise the SFE in Al_xCoCrFeNi, while Co and Cr suppress it. This conclusion is not only consistent with the Al trend presented in Fig. 2c and d, but also agrees with previous works done by Zaddach et al. [24] and Patriarca et al. [25]. They found that the SFE depended on the concentration of Co, Cr and Ni in FeNiCoCrMn HEA, which was similar to what we predicted. To further validate Eq. (2), the compositions in Table

S1 were substituted into Eq. (2), yielding an average SFE of -7.66 (mJ/m²), which was in good agreement with the average value calculated by DFT (-9.12 mJ/m²). Moreover, Eq. (2) was verified by using the bulk composition rather than the stacking fault composition. Table S2 shows the evaluated SFEs and the average SFEs calculated by DFT for Al_xCoCrFeNi. The predictions based on Eq. (2) are reasonably good compared to DFT results. This provides a convenient way to design and screen the HEAs with the improved mechanical properties. It is worth noticing that the estimate accuracy of the equation could be improved by using higher order polynomials, but it needs much more DFT data to obtain the coefficients. The current linear relationship (Eq. (2)) is good enough to identify the potential HEAs within a certain composition range (e.g., between 15% and 35%), as discussed below.

With Eq. (2), we are able to predict and determine the lowest SFE by adjusting the amount of the component for Al_xCoCrFeNi. If one wants to design an Al_xCoCrFeNi HEA with high strength but low SFE (high toughness), the easiest way is to add more Al and alter the composition of the other four elements based on Eq. (2). Take Al_{0.5}CoCrFeNi for instance. Being an element of matrix, the amount of these transition metals must be comparable with the amount of Al. Besides, according to Yeh's definition [1-3], the amount of each component in HEAs should be lower than 35 at%. Thus, we set up a concentration between 15% and 35% for the transition metals Co, Cr, Fe and Ni, and applied a linear programming to determine the composition showing the lowest SFE for x = 0.5. The optimized formula is $Al_{16}Co_{34}Cr_{50}Fe_{22}Ni_{22}$ and the evaluated SFE is -20.13 mJ/m², which is very low SFE compared to Al_{0.5}CoCrFeNi. Again, to ensure that our equation is valid for various compositions, we calculated the SFEs for 5 models with different atomic distributions and show that the average SFE calculated by DFT for $Al_{16}Co_{34}Cr_{50}Fe_{22}Ni_{22}$ is -16.85 mJ/m², which is approximate to the evaluated value.

Temperature strongly affects the mechanical properties of metals and alloys. It was observed that HEAs exhibited surprisingly large elongation at cryogenic temperature down to 77 K [26–28]. Otto et al. [28] proposed an idea indicating that the FCC-to-HCP

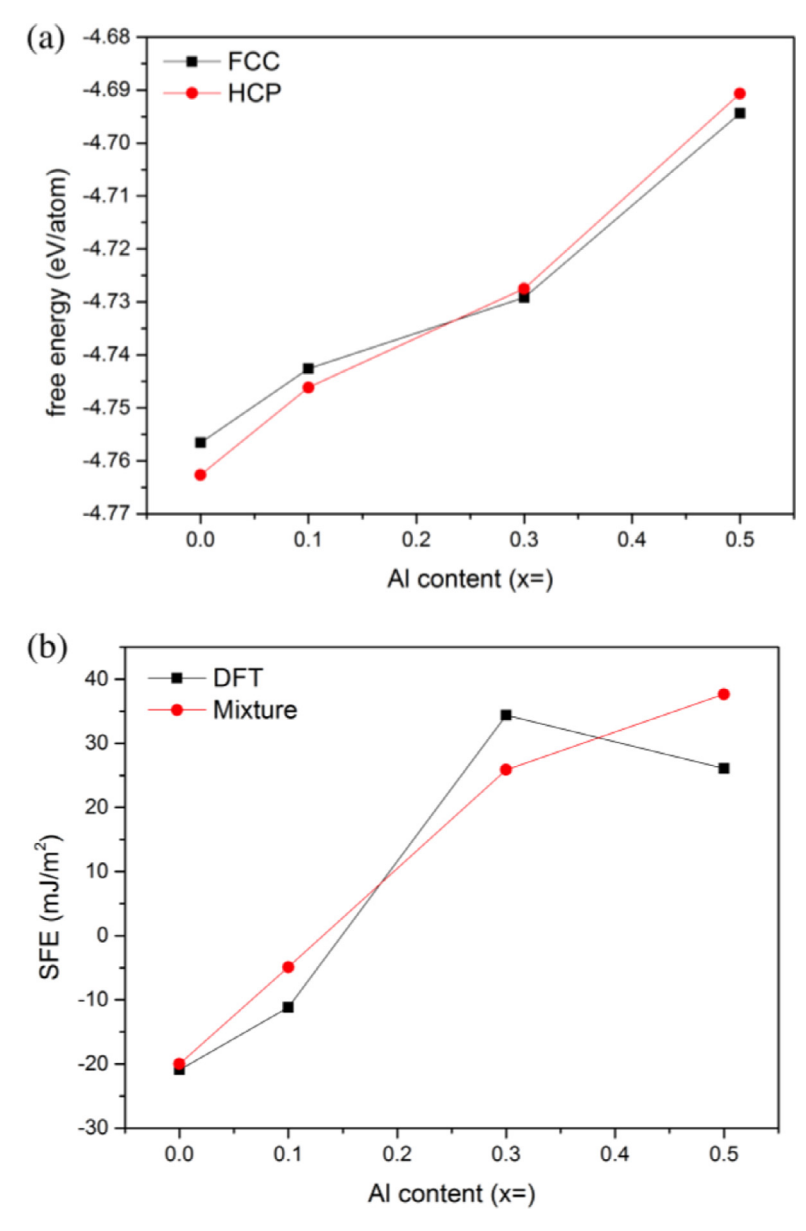


Fig. 4. (a) The free energy of FCC and HCP calculated by DFT as a function of Al composition. (b) The SFE, calculated by DFT and the energy mixture of FCC and HCP (in Fig. 4a), as a function of Al composition.

transformation was more likely to occur at lower temperature and the stacking fault and twinning process for a FCC-based HEA were exactly completed by this transformation. Thus, the observation of large elongation at low temperature was able to prove that the formation of stacking faults and twins were facilitated by a low temperature. In order to directly understand how much the temperature can influence the SFE in HEA, we carried out the abinitio molecular dynamics in VASP and used the Langevin thermostat [29] and Parrinello and Rahman [30,31] method to generate an NPT-ensemble. SFEs were derived at 300 K by using the models for 0K calculations (Fig. S5a and b). Since the temperature fluctuation is severe for both perfect and stacking models, we selected a temperature difference of 1 K as a tolerable value, causing merely \pm 1.55 mJ/m² error in SFE based on the DFT results. The SFEs for different atomic configurations at room temperature for CoCrFeNi are shown in Fig. S5d. As we can see, the SFE at 300 K shows higher value than SFE at OK and the average increase in SFE is $7.92 \pm 6.02 \text{ mJ/m}^2$. The results are consistent with Otto's speculation stating that if the SFE increases with increasing temperature,

the propensity of TWIP is lowered. Our results confirm that the SFE has positive correlation with temperature and are able to explain the observed phenomenon of decreasing elongation at higher temperature.

In summary, we have calculated the cohesive, vacancy, stacking fault and twin formation energies of Al_xCoCrFeNi high-entropy alloys. Our results show that local atomic configuration plays a critical role in determining the mechanical behavior of the HEAs. The structural stability and low diffusivity are mainly caused by the large variations of atomic configurations in HEAs and the SFE and TFE were extremely sensitive to the local atomic configuration. The experimentally observed local dissociation of dislocation in HEAs can be well explained by the LAC as a core effect. Negative SFE originates from the HCP structure having lower free energy than FCC structure at 0 K. Furthermore, the effect of temperature on SFE was investigated and our findings suggested that there was a positive correlation between SFE and temperature. Thus, the FCC-to-HCP transformation is more likely to occur at cryogenic temperature and our results are consistent with the experimental results

that elongation and tensile strength increase simultaneously for HEAs at 77 K. An accurate equation for the evaluation of SFE was derived by assuming the linear dependence between the SFE coefficients and the compositions. An AlCoCrFeNi HEA with desired properties can be successfully designed by using such approach.

Declaration of Competing Interest

The authors declare that they have no known competing financial interests or personal relationships that could have appeared to influence the work reported in this paper.

Acknowledgment

This work was supported by U.S. National Science Foundation (1762545, 1662288), and Army Research Lab (ARL) with Cooperative agreement number W911NF-16-2-0189.

Supplementary materials

Supplementary material associated with this article can be found, in the online version, at doi:10.1016/j.scriptamat.2019.11.016.

References

- [1] J.W. Yeh, S.K. Chen, S.J. Lin, J.Y. Gan, T.S. Chin, T.T. Shun, et al., Adv. Eng. Mater. 6 (5) (2004) 299–303.
- [2] J.W. Yeh, Ann. Chim. Sci. Matér. 31 (6) (2006) 633-648.
- [3] J.W. Yeh, JOM 65 (12) (2013) 1759–1771.
- [4] Y. Zhang, T.T. Zuo, Z. Tang, M.C. Gao, K.A. Dahmen, P.K. Liaw, et al., Prog. Mater. Sci. 61 (2014) 1–93.

- [5] B. Cantor, I.T.H. Chang, P. Knight, A.J.B. Vincent, Mater. Sci. Eng. A 375–377 (2004) 213–218.
- [6] K.Y. Tsai, M.H. Tsai, J.W. Yeh, Acta Mater. 61 (2013) 4887–4897.
- [7] N. Kumar, Q. Ying, X. Nie, R.S. Mishra, Z. Tang, P.K. Liaw, et al., Mater. Des. 86 (2015) 598–602.
- [8] W.R. Wang, W.L. Wang, S.C. Wang, Y.C. Tsai, C.H. Lai, J.W. Yeh, Intermetallics 26 (2012) 44–51.
- [9] Y.F. Kao, T.J. Chen, S.K. Chen, J.W. Yeh, J. Alloys Compd. 488 (2009) 57-64.
- [10] W.R. Wang, W.L. Wang, J.W. Yeh, J. Alloys Compd. 589 (2014) 143-152.
- [11] Z. Li, S. Zhao, H. Diao, P.K. Liaw, M.A. Meyers, Sci. Rep. 7 (2017) 42742.
- [12] G. Kresse, J. Hafner, Phys. Rev. B 47 (1993) 558.
- [13] G. Kresse, J. Furthmüller, Phys. Rev. B 54 (1996) 11169.
- [14] G. Kresse, J. Furthmüller, Comput. Mater. Sci. 6 (1996) 15-50.
- [15] P.E. Blöchl, Phys. Rev. B 50 (1994) 17953.
- [16] G. Kresse, D. Joubert, Phys. Rev. B 59 (1999) 1758.
- [17] J.P. Perdew, K. Burke, M. Ernzerhof, Phys. Rev. Lett. 78 (1997) 1396.
- [18] H.J. Monkhorst, J.D. Pack, Phys. Rev. B 13 (1976) 5188.
- [19] Q. Ding, Y. Zhang, X. Chen, X. Fu, D. Chen, S. Chen, et al., Nature 574 (2019) 223–227.
- [20] R. Liu, Z.J. Zhang, L.L. Li, X.H. An, Z.F. Zhang, Sci. Rep. 5 (2015) 9550.
- [21] D. Barbier, N. Gey, S. Allain, N. Bozzolo, M. Humbert, Mater. Sci. Eng. A 500 (2009) 196–206.
- [22] Z. Li, K.G. Pradeep, Y. Deng, D. Raabe, C.C. Tasan, Nature 534 (2016) 227–230.
- [23] Y. Deng, C.C. Tasan, K.G. Pradeep, H. Springer, A. Kostka, D. Raabe, Acta Mater. 94 (2015) 124–133.
- [24] A.J. Zaddach, C. Niu, C.C. Koch, D.L. Irving, JOM 65 (12) (2013) 1780–1789.
- [25] L. Patriarca, A. Ojha, H. Sehitoglu, Y.I. Chumlyakov, Scr. Mater. 112 (2016) 54–57.
- [26] D.Y. Li, Y. Zhang, Intermetallics 70 (2016) 24-28.
- [27] B. Gludovatz, A. Hohenwarter, D. Catoor, E.H. Chang, E.P. George, R.O. Ritchie, Science 345 (6201) (2014) 1153–1158.
- [28] F. Otto, A. Dlouhy, Ch. Somsen, H. Bei, G. Eggeler, E.P. George, Acta Mater. 61 (2013) 5743–5755.
- [29] M.P. Állen, D.J. Tildesley, Computer Simulation of Liquids, Oxford University Press, New York, 1991.
- [30] M. Parrinello, A. Rahman, Phys. Rev. Lett. 45 (1980) 1196.
- [31] M. Parrinello, A. Rahman, J. Appl. Phys. 52 (1981) 7182.